International Journal of Pharmaceutical Research and Applications
Volume 10, Issue 3 May–June 2025, pp: 311-320 www.ijprajournal.com ISSN: 2456-4494

Formulation Development and characterization of Quercetin Loaded Nanoemulsion

Arpita Chaudhary*[1], Dr. Vivek Gupta[2], Nida Musheer[3], Gyan Singh[4]
[1] PG Research Scholar, Faculty of Pharmacy, P.K University, Thanara, Shivpuri, M.P, India
[2] Professor, Faculty of Pharmacy, P.K University, Thanara, Shivpuri, M.P, India
[3]Assistant Professor, Faculty of Pharmacy, P.K University, Thanara, Shivpuri, M.P, India
[4]Associate Professor, Faculty of Pharmacy, P.K University, Thanara, Shivpuri, M.P, India

Date of Submission: 01-05-2025 Date of Acceptance: 10-05-2025

ABSTRACT
The major limitations of quercetin delivery, including solubility and bioavailability, can be effectively overcome by encapsulating it into a precise nanoemulsion system. Optimized quercetin-loaded nanoemulsion exhibited improved solubility, permeability, biocompatibility, oral bioavailability, and stability with multifaceted therapeutic applications. Applications for quercetin have been restricted because of its weak water solubility and high sensitivity to chemical degradation. In order to use quercetin as a functional food component, this study assessed the hypocholesterolemic activity of quercetin and quercetin-loaded nanoemulsion (NQ) and examined the effects of pH on the production of NQ. The NQ particle size ranged from 207 to 289 nm, with a polydispersity index of less than 0.47. As the pH rose from 4.0 to 9.0, the encapsulation effectiveness gradually improved from 56 to 92%. During three months of storage at 21 and 37 °C, NQ demonstrated good stability in the pH range of 6.5 to 9.0.

Keywords: Nanoemulsion, bioavailability, biocompatibility, polydispersity.

I. INTRODUCTION

Nanotechnology is the study of materials that are engineered at the nanoscale, typically with sizes between 1 and 100 nm and sometimes up to 1000 nm. Because of their size, these nanomaterials frequently display a wide range of physical, chemical and biological characteristics that allow their innovative uses [1]. These particles frequently provide greater stability, more efficiency, and less harmful effects as compared to the pharmaceutical macromolecules that are already on the market. Because of their enhanced adaptability, biocompatibility, and biodegradable properties, lipid nanoparticles have drawn particular interest [2]. Based on particular composition and physicochemical characteristics these lipid nanoparticles have been classified as liposomes, solid lipid nanoparticles, nanoemulsions and also self-emulsifying drug delivery systems. These nanocarriers are considered as efficient delivery systems for sparingly soluble drugs, which comprises 40% of new chemical entities [3]. Uncontrolled drug release has been identified as a significant problem for SEDDS; even hydrophobic and lipophilic medications that are highly soluble in the oily medium of the globules that SEDDS generate cannot be fully released [4]. In addition, SEDDS as liquid formulations have shown a number of drawbacks, such as reduced drug loading, drug escape, decreased stability, and a restricted uptake of dose forms [5]. In contrast, nanoemulsions have become a viable medication delivery technology because of their unique characteristics. Kinetically stable liquid/liquid dispersions are often defined as nanoemulsions with droplet sizes less than 200 nm.

1.1 Quercetin

Quercetin belongs to the flavonoid category of polyphenols and is a plant flavonol. Many fruits, vegetables, leaves, seeds, and grains contain it; notable foods that contain significant levels of it include kale, red onions, and capers. It is utilized as a component in meals, drinks, and dietary supplements and has a bitter taste. Quercetin appears as yellow needles or yellow powder. Converts to anhydrous form at 203-207 °F. Alcoholic solutions taste very bitter. Quercetin is a pentahydroxyflavone having the five hydroxy groups placed at the 3-, 3'-, 4'-, 5- and 7-positions. It is one of the most abundant flavonoids in edible vegetables, fruit and wine. It has a role as an antibacterial agent, an antioxidant, a protein kinase inhibitor, an antineoplastic agent, an EC 1.10.99.2 [ribosyldihydronicotinamide dehydrogenase (quinone)] inhibitor, a plant metabolite, a

International Journal of Pharmaceutical Research and Applications
Volume 10, Issue 3 May–June 2025, pp: 311-320 www.ijprajournal.com ISSN: 2456-4494

phytoestrogen, a radical scavenger, a chelator, an Aurora kinase inhibitor and a geroprotector. It is a pentahydroxyflavone and a 7-hydroxyflavonol. It is a conjugate acid of a quercetin-7-olate. Quercetin is a flavonol widely distributed in plants. It is an antioxidant, like many other phenolic heterocyclic compounds. Glycosylated forms include RUTIN and quercetrin.

1.2 Methods for the Preparation of Nanoemulsion-Based Systems

Various methods and experimental techniques have been developed for the preparation of nanoemulsion-based delivery systems, mainly categorized as low-energy and high-energy [6]. The selection of an apt method for the preparation of nanoemulsions depends on the characteristics of the compounds (specifically the surfactant and oil phases), as well as the required physicochemical attributes and operational qualities of the ultimate product (including rheological, optical, release, and stability properties) [7,8]. Understanding the various fabrication methods is crucial for relevant personnel to choose the most suitable preparation technique and fabricate nanoemulsions for special application.

1.3 In-Vitro Characterization Techniques of Nanoemulsion

While fabricating nanoemulsions, size determination is mandatorily done, so adherence to a strict droplet size is a prerequisite as the droplet size influences numerous parameters. Polydispersity index; an important parameter that measures the droplet size distribution uniformity. The numerical value of PDI below 1.0 is considered as “monodisperse” and more is considered as “polydisperse”, however, in lipid-based carriers used in drug delivery, a PDI of 0.3 and below is considered to be acceptable, indicating homogenous system [9]. Particle size analysers measures droplet size either using laser diffraction or using photon correlation spectroscopy (PCS) [10].

Further characterization of nanoemulsions using optical tools aided in measurement of parameters such as refractive index, and static light scattering. Refractive index is measured using a refractometer, while diffusing-wave spectroscopy is used to analyse thick concentrated samples. Zeta potential measurements provides a clear picture about the formulation’s long-term stability as well as of any possible interactions with the target matrix. For a nanoemulsion to be considered as stable for long term, zeta potential values between +30 mV or −30 mV is considered as good. It is possible to portray the conformational changes occurring in the molecules that makes up the nanoemulsion using a combination of zeta potential measurements, fluorescence quenching, and absorption spectroscopy. It can help in delineating the changes with respect to alterations in drug loading, pH, temperature and other processing variables [11,12]

II. MATERIAL & METHODS:

Quercetin (95%) was purchased from Sigma Aldrich Chemicals, USA. Capmul MCM (CAP MCM), Capmul MCM NF (CAP MCM NF), and Capryol PGMC (CAP PGMC) were gifted samples from Gattefosse (Saint-Priest, Cedex, France). Cremophor RH40 (CR RH 40), Cremophor ELP (CR ELP), and Transcutol HP (TRANS HP) were generously gifted from BASF (Ludwigshafen, Germany). Milli-Q water was used in all experiments. All other chemicals and reagents used were of analytical grade.

Methodology:

Preparation of PCL Nanoparticles: In this the nanoparticles are prepared by solvent evaporation method. Initially a weighed quantity of poloxamer-188 is added to double distilled water with magnetic stirring. The solution was maintained at 50-600 C and the PCL was dissolved in acetone with mild sonication4 . Then organic solution was added to the aqueous solution slowly using micro pipette to disperse the organic solution. Immediately on addition of PCL to aqueous solution it forms a bluish tinge which indicates the formation of nanoparticles. This solution is then stirred for about 2 hrs at the same temperature.[13-14] Then the nanoparticles are recovered by centrifugation at low pressure above 10,000 rpm. The formed sediment is then lyophilized to form nanoparticles.

III. OPTIMIZATION STUDIES:

3.1 Analytical Method Development Using UV Spectroscopy

A double beam UV-Visible Spectrophotometer-1800 (Shimadzu, Japan) with UV probe software (version 2.41) was used to measure and record the absorption spectra. The samples were scanned over the range of 200.0 nm to 400.0 nm to obtain the absorption maxima of the solute (λmax). QT was insoluble in phosphate buffer solution (pH 7.4), so we used methanolic

International Journal of Pharmaceutical Research and Applications
Volume 10, Issue 3 May–June 2025, pp: 311-320 www.ijprajournal.com ISSN: 2456-4494

phosphate buffer solution (pH 7.4). Optimization of the methanolic content in the solution was achieved by making phosphate buffer solution (100 mL) with varying percentage of methanol and further the pH of the medium was adjusted to pH 7.4. Precipitation was checked for 36 hrs to ensure solubility in prepared media. The absorbance of the test samples varied concentrations was obtained at the wavelength of absorption maximum.

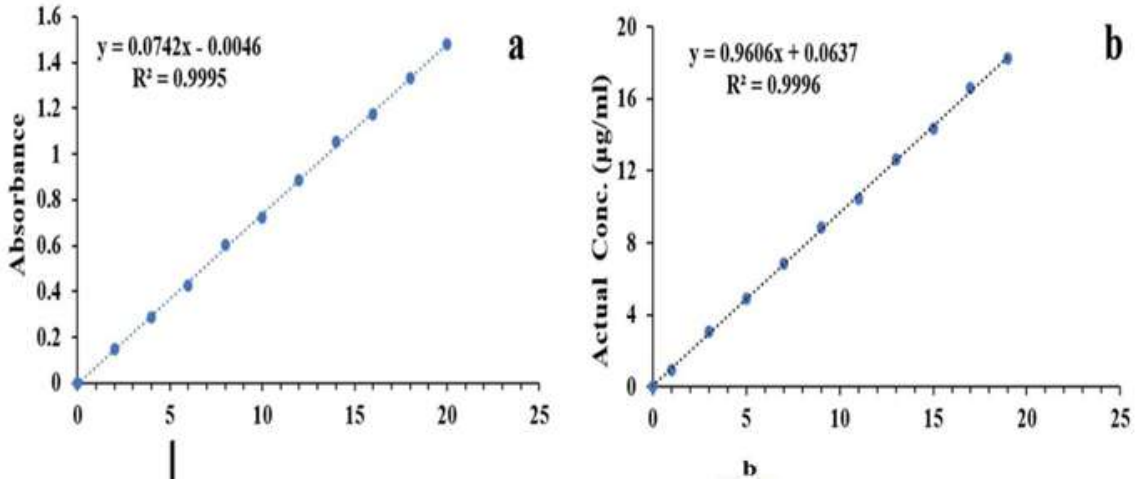

Figure-1 Standard plot (a) and contemplation plot (b) of quercetin in methanol.

3.2 Solubility Studies

Solubility studies were performed by using the shaking water bath method. An excess quantity of QT was added to 2 g of different oils (CAP MCM, CAP MCM NF, and CAP PGMC), surfactants (CR RH 40 and CR ELP), and co-surfactants (PEG 400 and TRANS HP). Mixtures of QT and excipients were first vortexed (REMI CM-101, India) to facilitate the mixing of QT with excipients, and the mixtures were then allowed to reach equilibrium at 37 ± 3 °C in a shaking water bath (REMI RSB-12, India). After 48 h, all the test mixtures were centrifuged (Eppendorf AG, Germany) at 12,000g for 15 min to separate undissolved QT, followed by filtration through a 0.45 µm membrane filter. Further, the filtrates were diluted with methanol and the concentration of QT was determined using a UV/Vis spectrometer (UV-1800, Shimadzu, Japan) at 371.4 nm based on a standard curve of known QT concentrations (y = 0.0742x - 0.0046; r2=0.995) [15].

Amongst various excipients explored, solubility of QT was found maximum in CAP MCM NF (oil, 20.35 mg/g), CR RH 40 (surfactant, 164.3 mg/gm) and TRANS HP (co-surfactant, 133.68 mg/gm). During the solubility study, the color of QT changed in presence of TRANS HP, hence it was not considered in nanoemulsion formulation[16]. Furthermore, we have used only CAP MCM and CR RH 40 as oil and surfactant, respectively, as the addition of co-surfactant had no significant impact on the desired attributes (lower PS and higher ZP) of QTNE.

International Journal of Pharmaceutical Research and Applications
Volume 10, Issue 3 May–June 2025, pp: 311-320 www.ijprajournal.com ISSN: 2456-4494

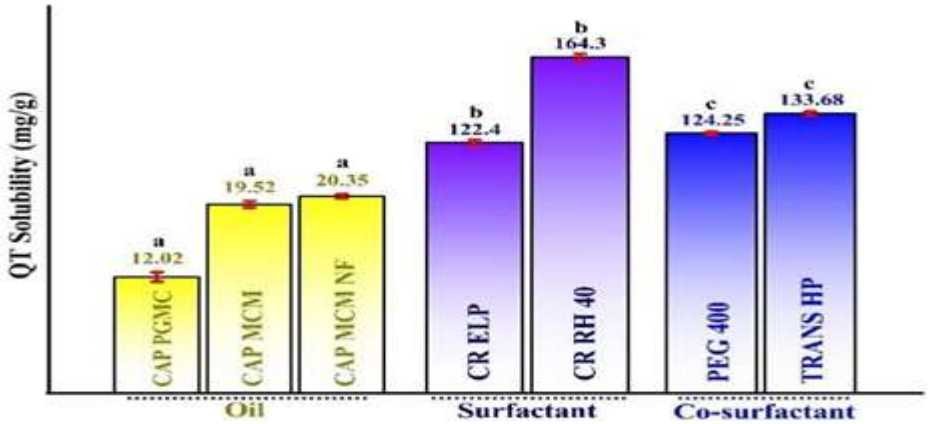

Figure 2 Solubility of quercetin in various excipients (oils, surfactants, and cosurfactants).

3.3 FTIR studies

FTIR helps to establish the intermolecular interaction between drug and excipients. The FTIR spectra of pure QT (Figure 3) showed major characteristic peaks as broad phenolic –OH stretching (3397 cm-1), –CH stretching (2717 cm-1), –C=O stretching (1606 and 1665 cm-1), –C=C symmetric stretching (1433 and 1523 cm-1), –CH bending (1366 cm-1), -C-O-C stretching (1111 cm-1) and = CH bending (830 cm-1) (Das et al., 2020).

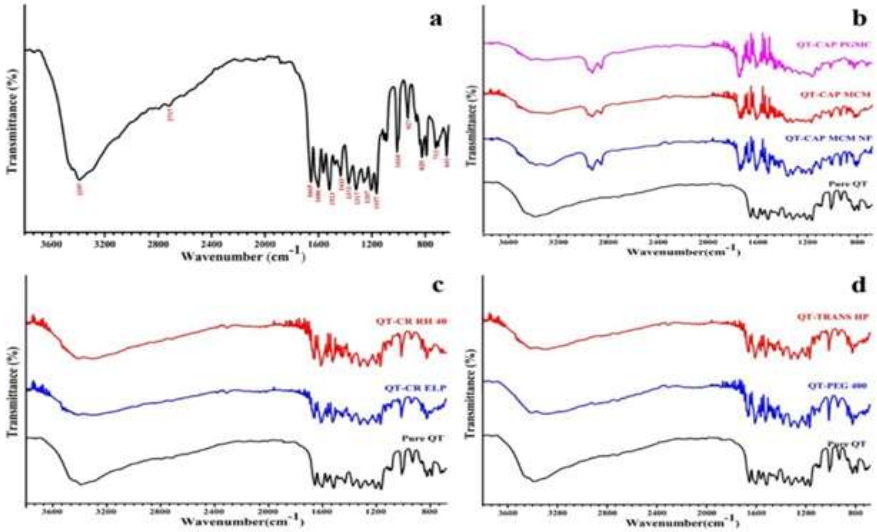

Figure 3 FTIR spectra of pure QT(a), dried residues of QT-O(b), QT-CS(c) and QT-S(d).

3.4 RAMAN studies:

Raman spectroscopy is a non-destructive analytical method that is extensively useful for the physicochemical characterization of chemical compounds in general and pharmaceuticals, in particular [17]. Furthermore, in contrast to IR spectroscopy, it is not disturbed by the presence of water [18].

International Journal of Pharmaceutical Research and Applications
Volume 10, Issue 3 May–June 2025, pp: 311-320 www.ijprajournal.com ISSN: 2456-4494

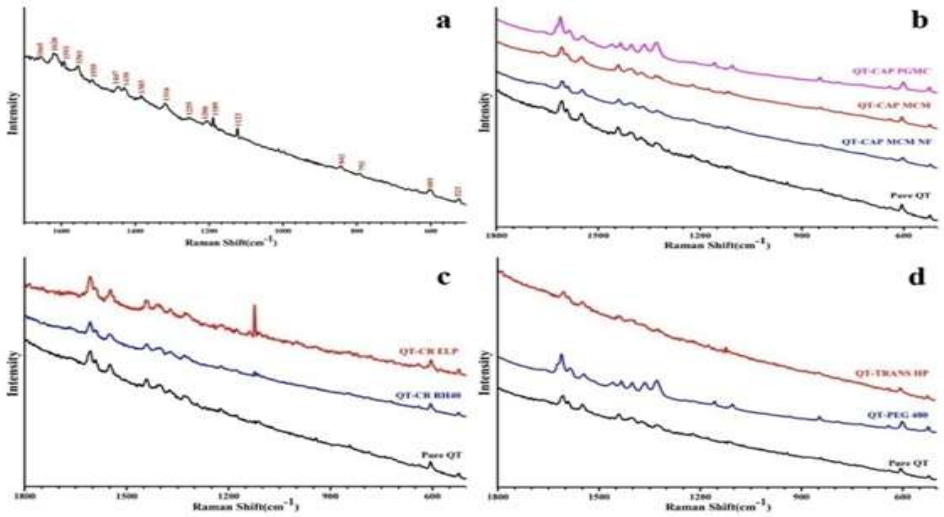

Figure 4 Raman spectra of pure QT(a), dried residues of QT-O(b), QT-S(c) and QT-CS(d).

The Raman spectra of pure QT (Figure 4) showed major characteristic peaks at 1666 cm-1 (C4=O2 stretching), 1618 cm-1 (C2=C3 stretching; C3/C5–OH bending), and less intense peaks at 1593 and 1554 cm-1 (C=O stretching and C-C stretching of ring B). Other major peaks at 1474 cm−1 (C3/C5/C7–OH and C6/C8–H bending), 1424 cm-1, 1382 cm-1, and 1318 cm-1 (C5/C7-OH bending ring A), 1333 cm-1 (C3-OH bending of ring C), 1142 cm-1 (C7-OH and C-C-H bending of ring A) and 1123 cm-1 (C3-OH, C3′-OH, C4′-OH, and C-C-H bending) were observed.

3.5 DSC-TG studies

DSC-TG thermograms of pure QT, dried residues of QT-O, QT-S and QT-CS is illustrated in Figure 5. DSC curves of pure QT (Figure 5) indicated one endothermic peak at 115 °C, due to moisture loss, one sharp endothermic peak at 322.2 °C, related to its melting point and one exothermic peak at 348.4 °C, due to its decomposition. TG curves demonstrated two weight loss stages of pure QT appearing in the range of 77.6-124.1 °C and 286.9-372.3 °C, attributing to moisture loss and structure degradation. Similar results were reported in previous studies [19]. As shown in Figure 5(b-d), DSC-TG thermograms of dried residues of QT-O, QT-S, and QT-CS were found to be similar as that of pure QT (Figure 5a) except dried residue of QT-CAP PGMC.

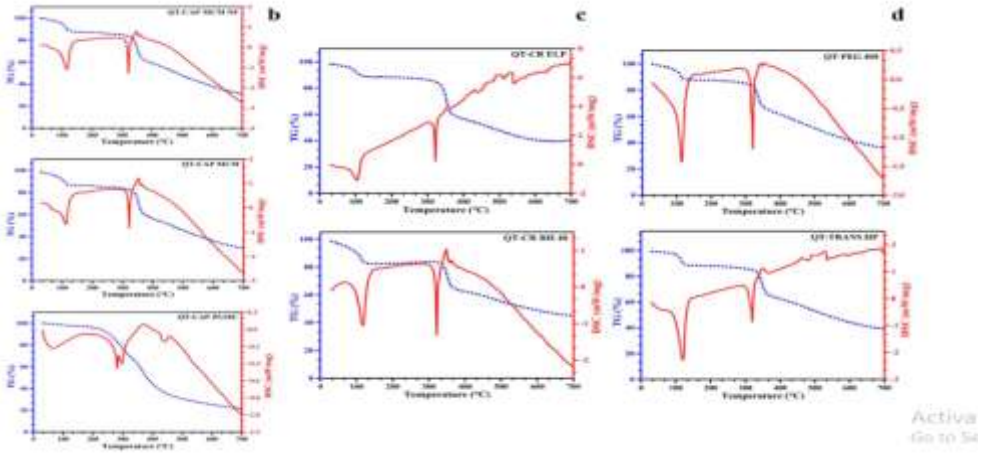

Figure 5 DSC-TG the rmograms of pure QT (a), dried residues of QT-O (b), QT-S (c) and QT-CS (d).

International Journal of Pharmaceutical Research and Applications
Volume 10, Issue 3 May–June 2025, pp: 311-320 www.ijprajournal.com ISSN: 2456-4494

3.6 P-XRD studies:

XRD patterns for pure QT, dried residues of QT-O, QT-S and QT-CS is shown in Figure 7.8. The intense peaks (Figure 6a) at 10.44°, 14.12°, 17.92°, 24.14°, 26.41°, 28.27° and 30.51°, indicated the crystalline nature of QT. Similar results were reported in previous studies [20-21]. XRD pattern of dried residues of QT-O, QT-S and QT-CS were found to be similar as that of pure QT (Figure 6a) except for dried residue of QT-CR ELP (Figure 6c) and QT-TRANS HP (Figure 6d), in which peaks shifting were observed.

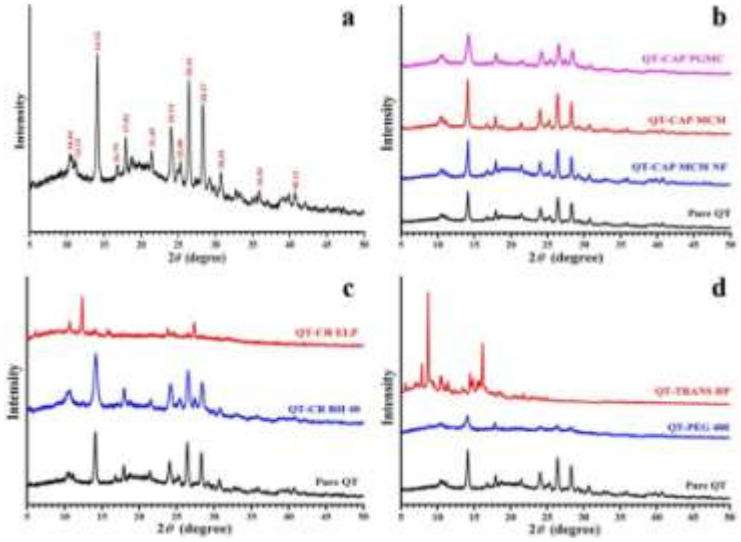

Figure 6 PXRD diffractograms of pure QT(a), dried residues of QT-O (b), QT-S (c) and QT-CS (d).

3.7 FESEM studies

The FESEM micrograph of pure QT (Figure 7a) elucidated the existence of crystalline particles in native form with rough and cylindrical crystal habit. Similar findings were also reported by [22-23]. From the micrographs of QT-CAP MCM NF (Figure 7b) and QT-CAP MCM (Figure 7c), it was evident that the QT was distributed with a high degree of homogeneity and a smoother crystal surface. In case of QT-CAP PGMC (Figure 7d), some particles existed in agglomerated form and some particles were in a dissolved state (dotted part) [24].

The micrographs of QT-CR ELP (Figure 7e) showed the agglomeration and dissolved state of the drug (dotted part). QT-CR RH 40 (Figure 7f) showed a similar pattern as that of pure drug. However, particle surface was observed to be smoother and denser suggesting particle-particle adherence. The dried residues of QT-PEG 400 (Figure 7g) showed smooth surface with an apparent PEG 400 layer, while the surface of QT-TRANS HP (Figure 7h) showed same patterns as QT-CR ELP.

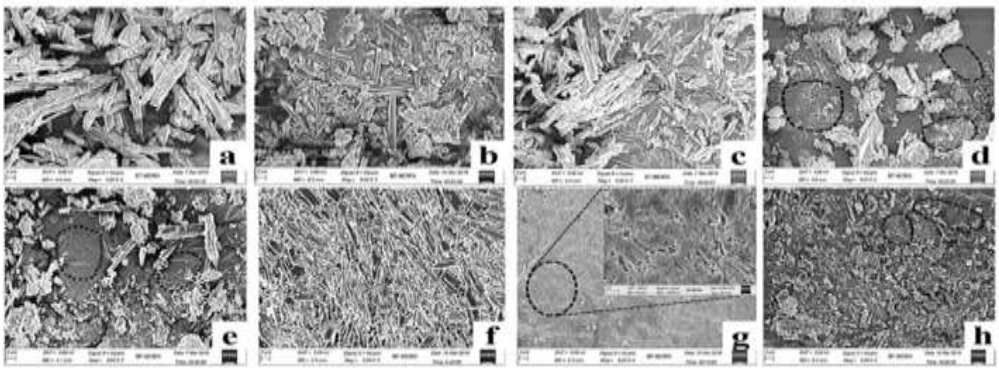

Figure 7 FESEM micrographs of pure QT(a), dried residue of QT-CAP MCM NF(b), QT-CAP MCM(c), QT-CAP PGMC(d), QT-CR ELP(e), QT-CR RH 40(f), QT-PEG 400(g) and QT-TRANS HP(h).

International Journal of Pharmaceutical Research and Applications
Volume 10, Issue 3 May–June 2025, pp: 311-320 www.ijprajournal.com ISSN: 2456-4494

IV. CHARACTERIZATION STUDIES

Oil and surfactant concentration are important parameters affecting the particle size of the formulation. In the present study, the varying concentrations of oil and surfactant were selected based on preliminary studies. Based on mixture design (simplex-lattice design), the factor combinations of CAP MCM NF (X1) and CR RH 40 (X2) resulted different response for the mean particle size (Y1), zeta potential (Y2) and polydispersity index (Y3) of formulations (QN1-QN7).

4.1 Particle Size Analysis

The results of the two-component mixture plot (Figure 8a) showed that the ratio of oil (X1) and surfactant (X2) exhibited significant effects on the particle size (Y1). It was noticed that the particle size (Y1) of the formulations linearly increased with the increasing proportion of oil (X1) beyond 250 mg. In contrary, particle size decreased with increasing content of surfactant (Figure 8a). The equal factor concentration of oil and surfactant gave minimum particle size range as shown in Figure 8a. In addition, Figure The results of the two-component mixture plot (Figure 8a) showed that the ratio of oil (X1) and surfactant (X2) exhibited significant effects on the particle size (Y1). It was noticed that the particle size (Y1) of the formulations linearly increased with the increasing proportion of oil (X1) beyond 250 mg. In contrary, particle size decreased with increasing content of surfactant (Figure 8a). The equal factor concentration of oil and surfactant gave minimum particle size range as shown in Figure 8a. In addition, Figure 8b portrays the predicted versus actual response outcomes, wherever all the data points are scattered along the straight-line justifying goodness of fit (r2=0.9945).

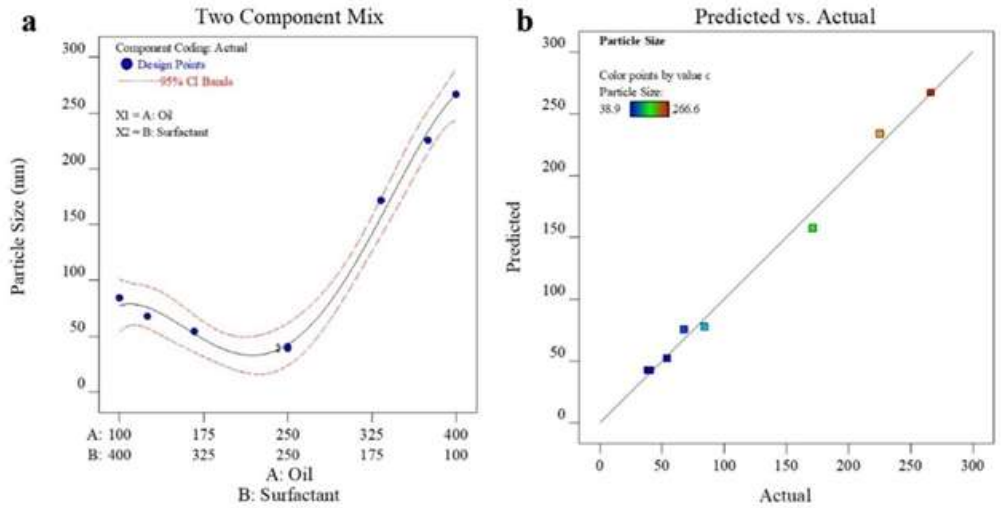

Figure 8 Response plots for particle size (Y1) of two-component mixture plot (a) and predicted vs. actual values (b).

4.2 Zeta potential analysis

The zeta potential is a key factor in the stability of colloidal dispersions. The magnitude of the zeta potential indicates the degree of electrostatic repulsion between adjacent, similarly charged particles in the dispersion. The zeta potential of nanoemulsions ranged from -12.14 ± 0.48 to -23.37 ± 0.43 mV in aqueous media (Milli-Q water) . Results showed that the overall charge over the globules of all nanoemulsions is negative. Mathematical models were generated us ing Design-Expert® 13.0.3.0 software (Stat-Ease, Inc., USA), for the considered response variables, are tabulated. The reduced coded equation derived using the best fit mathematical model to relate the response Y2 and the independent variables is given in Eqn.: Y2 = -23.21X1 - 13.04X2

4.3 Stability Studies

Optimized quercetin nanoemulsion (QTNE) stored at 4°C was monitored for alterations in the particle size, zeta potential and polydispersity index with a time interval upto 90 days. It was observed that the PS, ZP and PDI values of optimized QTNE varied from 38.9 to 54.11 nm, -18.51 to - 23.19 mV and 0.278 to 0.327,

International Journal of Pharmaceutical Research and Applications
Volume 10, Issue 3 May–June 2025, pp: 311-320 www.ijprajournal.com ISSN: 2456-4494

respectively, indicating relatively narrow particle size distribution and stable nanoemulsion (Figure 9).

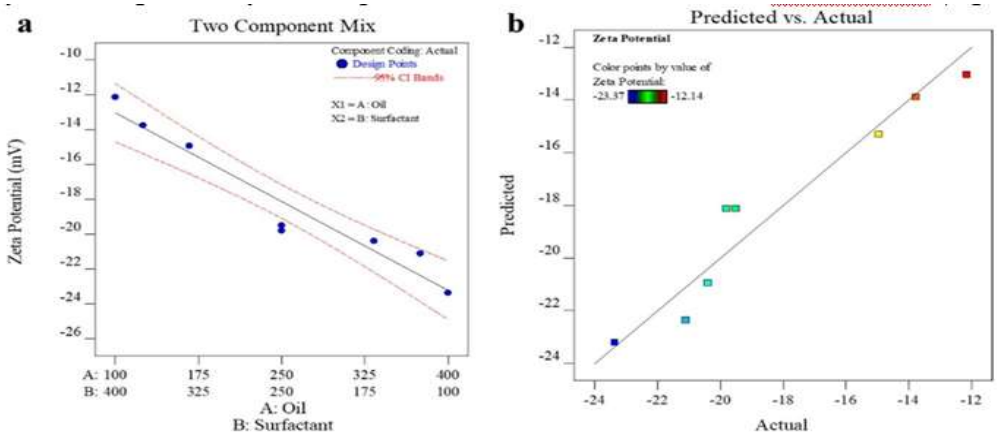

Figure 9 Stability assessment of particle size (nm), zeta potential (mV) and polydispersity index values of optimized QTNE stored at 4 °C. Different small case letters indicate significant difference between the days ($p < 0.05$) and different capital case letters indicates no significant difference between the days ($p > 0.05$), n=3.

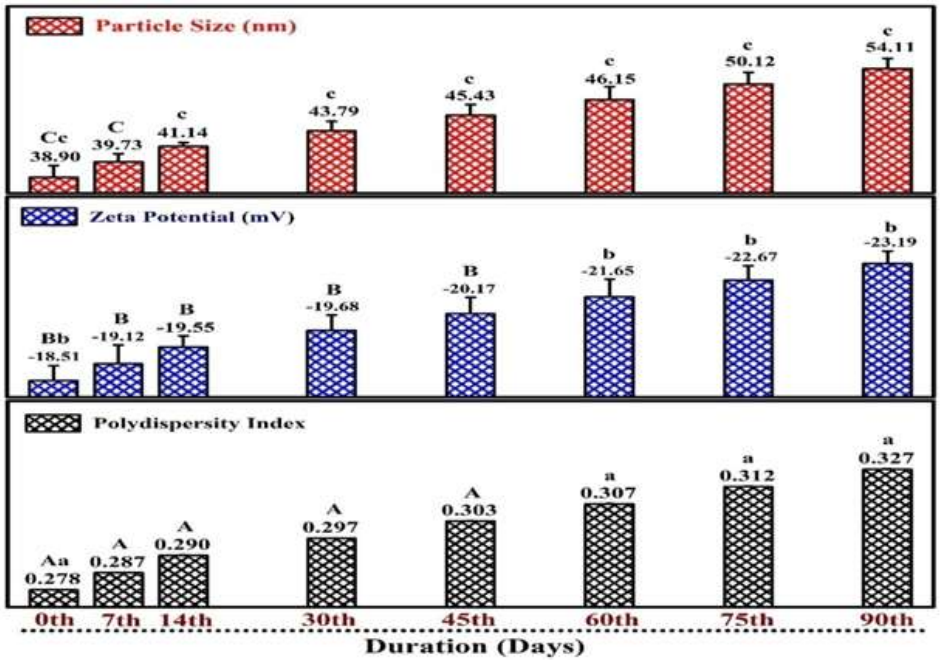

V. CONCLUSION:

Nanoemulsion systems have evolved as a potential approach in the field of Nanotechnology - based drug delivery approaches, however, there is still a gap to be filled to fully explain the yet to be resolute in the exploration of future medicine, particularly from laboratory developments to clinical translations. Conclusively, the envisage studies on nanoemulsion-based drug delivery systems of quercetin fabricated robust delivery systems and demonstrated their enhancement of permeation potential and oral bioavailability. Amongst various approaches, NEs are a promising strategy to enhance the solubility, stability, and oral bioavailability of QT. Moreover, incorporating quercetin in NE composed of foodgrade excipients has an advantage over other nanosystems due to its longer shelf life and greater stability in biological fluids without any adverse effects. The mixture design (simplex lattice) was used for the optimization and development of quercetin-loaded nanoemulsion. Prior to the preparation of QTNE,

International Journal of Pharmaceutical Research and Applications
Volume 10, Issue 3 May–June 2025, pp: 311-320 www.ijprajournal.com ISSN: 2456-4494

preformulation studies will conduct to select best oil and surfactant that showed no incompatibility with the drug. Selection of excipients will perform through various compatibility studies (FTIR, RAMAN, DSC-TGA, and PXRD) and surface morphology (FESEM). QTNE formulation will present appreciable results owing to their nanosized globules, higher absolute zeta potential, lower polydispersity index. In-vitro drug release studies showed that QTNE increase the QT release with sustained effect.

REFERENCE

[1]. Abbas, S., Hayat, K., Karangwa, E., Bashari, M., Zhang, X., 2013. An Overview of Ultrasound-Assisted Food-Grade Nanoemulsions. Food Engineering Reviews 5, 139-157.

[2]. Caddeo, C., Gabriele, M., Fernandez-Busquets, X., Valenti, D., Fadda, A.M., Pucci, L., Manconi, M., 2019. Antioxidant activity of quercetin in Eudragit-coated liposomes for intestinal delivery. Int J Pharm 565, 64-69.

[3]. Badawi, M.A., El-Khordagui, L.K., 2014. A quality by design approach to optimization of emulsions for electrospinning using factorial and D-optimal designs. Eur J Pharm Sci 58, 44-54.

[4]. Abrahamsson, B., Lennerna¨s, H., 2003. Application of the Biopharmaceutic Classification System Now and in the Future, in: Waterbeemd, H.V.D., Lennerna¨s, H., Artursson, P. (Eds.), Drug Bioavailability: Estimation ofSolubility, Permeability, Absorption and Bioavailability. WILEY-VCH Verlag GmbH & Co. KGaA, Weinheim, Weinheim, Germany.

[5]. Bachmann, L., 1987. Freeze-Etching of Dispersions, Emulsions and Macromolecular Solutions of Biological Interest, Cryotechniques in Biological Electron Microscopy, pp. 192-204.

[6]. Daina, A., Michielin, O., Zoete, V., 2017. SwissADME: a free web tool to evaluate pharmacokinetics, drug-likeness and medicinal chemistry friendliness of small molecules. Sci Rep 7, 42717.

[7]. Badawi, M.A., El-Khordagui, L.K., 2014. A quality by design approach to optimization of emulsions for electrospinning using factorial and D-optimal designs. Eur J Pharm Sci 58, 44-54.

[8]. Ahmadi Oskooei, F., Mehrzad, J., Asoodeh, A., Motavalizadehkakhky, A., 2021. Olive oil-based quercetin nanoemulsion (QuNE)'s interactions with human serum proteins (HSA and HTF) and its anticancer activity. J Biomol Struct Dyn, 1-14.

[9]. Das, S.S., Sarkar, A., Chabattula, S.C., Verma, P.R.P., Nazir, A., Gupta, P.K., Ruokolainen, J., Kesari, K.K., Singh, S.K., 2022. Food-Grade Quercetin-Loaded Nanoemulsion Ameliorates Effects Associated with Parkinson's Disease and Cancer: Studies Employing a Transgenic C. elegans Model and Human Cancer Cell Lines. Antioxidants (Basel)

[10]. Eftekhari, A., Ahmadian, E., Panahi-Azar, V., Hosseini, H., Tabibiazar, M., Maleki Dizaj, S., 2018. Hepatoprotective and free radical scavenging actions of quercetin nanoparticles on aflatoxin B1-induced liver damage: in vitro/in vivo studies. Artif Cells Nanomed Biotechnol 46, 411-420.

[11]. Ganachaud, F., Katz, J.L., 2005. Nanoparticles and nanocapsules created using the Ouzo effect: spontaneous emulisification as an alternative to ultrasonic and highshear devices. Chemphyschem 6, 209-216.

[12]. Fan, J., Chen, Y., Yan, H., Niimi, M., Wang, Y., Liang, J., 2018. Principles and Applications of Rabbit Models for Atherosclerosis Research. J Atheroscler Thromb 25, 213-220.

[13]. Gupta, A., Eral, H.B., Hatton, T.A., Doyle, P.S., 2016a. Nanoemulsions: formation, properties and applications. Soft Matter 12, 2826-2841.

[14]. Huang, M., Su, E., Zheng, F., Tan, C., 2017. Encapsulation of flavonoids in liposomal delivery systems: the case of quercetin, kaempferol and luteolin. Food Funct 8, 3198-3208.

[15]. Naseema, A., Kovooru, L., Behera, A.K., Kumar, K.P.P., Srivastava, P., 2021. A critical review of synthesis procedures, applications and future potential of nanoemulsions. Adv Colloid Interface Sci 287, 102318.

[16]. Pandey, S.K., Patel, D.K., Thakur, R., Mishra, D.P., Maiti, P., Haldar, C., 2015.

Anticancer evaluation of quercetin embedded PLA nanoparticles synthesized by emulsified nanoprecipitation. Int J Biol Macromol 75, 521-529.

[17]. Singh, B., Kumar, R., Ahuja, N., 2005. Optimizing drug delivery systems using systematic "design of experiments." Part I: fundamental aspects. Crit Rev Ther Drug Carrier Syst 22, 27-105.

[18]. Verma, N.K., Crosbie-Staunton, K., Satti, A., Gallagher, S., Ryan, K.B., Doody, T., McAtamney, C., MacLoughlin, R., Galvin, P., Burke, C.S., Volkov, Y., Gun'ko, Y.K., 2013. Magnetic core-shell nanoparticles for drug delivery by nebulization. Journal of nanobiotechnology 11, 1.

[19]. Parveen, R., Baboota, S., Ali, J., Ahuja, A., Vasudev, S.S., Ahmad, S., 2011. Oil based nanocarrier for improved oral delivery of silymarin: In vitro and in vivo studies. Int J Pharm 413, 245-253.

[20]. Narang, A.S., Delmarre, D., Gao, D., 2007. Stable drug encapsulation in micelles and microemulsions. Int J Pharm 345, 9-25.

[21]. Iyer, R., Petrovska Jovanovska, V., Berginc, K., Jaklic, M., Fabiani, F., Harlacher, C., Huzjak, T., Sanchez-Felix, M.V., 2021. Amorphous Solid Dispersions (ASDs): The Influence of Material Properties, Manufacturing Processes and Analytical Technologies in Drug Product Development. Pharmaceutics 13.

[22]. Choudhary, A., Kant, V., Jangir, B.L., Joshi, V.G., 2020. Quercetin loaded chitosan tripolyphosphate nanoparticles accelerated cutaneous wound healing in Wistar rats. Eur J Pharmacol 880, 173172.

[23]. Buranasuksombat, U., Kwon, Y.J., Turner, M., Bhandari, B., 2011. Influence of emulsion droplet size on antimicrobial properties. Food Science and Biotechnology 20, 793-800.

[24]. Ali, H., Prasad Verma, P.R., Dubey, S.K., Venkatesan, J., Seo, Y., Kim, S.-K., Singh, S.K., 2017. In vitro–in vivo and pharmacokinetic evaluation of solid lipid nanoparticles of furosemide using Gastroplus™. RSC Advances 7, 33314-33326.